ChemComm

Accepted Manuscript

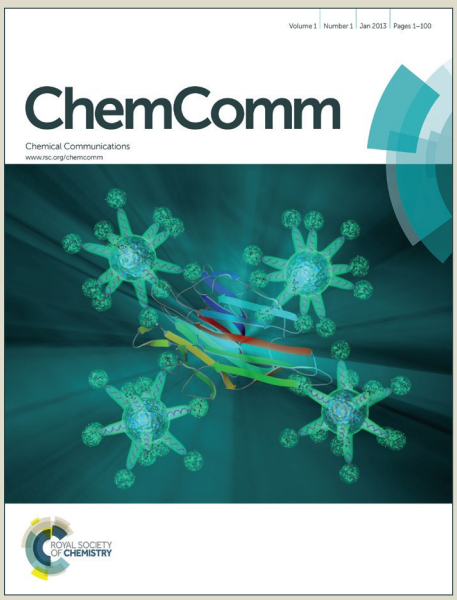

ROYAL SOCIETY OF CHEMISTRY

www.rsc.org/chemcomm

ChemComm

RSCPublishing

COMMUNICATION

Near-infrared Light-controlled System for Reversible Presentation of Bioactive Ligands Using Polypeptide-engineered Functionalized Gold Nanorods

Cite this: DOI: 10.1039/x0xx00000x

Received 00th January 2012,
Accepted 00th January 2012

DOI: 10.1039/x0xx00000x

www.rsc.org/

Jie Yang, Ming-Hao Yao, Ming-Shuo Du, Rui-Mei Jin, Dong-Hui Zhao, Jun Ma, Zhi-Ya Ma, Yuan-Di Zhao*, and Bo Liu*

A near-infrared light-controlled hybrid platform with polypeptide-engineered functionalized gold nanorods has been designed for reversible presentation of the immobilized ligands to cell surface receptors on the engineered materials.

Cell microenvironments of engineered biomaterials are the key factor to guide cell behavior and fate selection in tissue engineering and regenerative medicine.[1] Various types of biomaterials have been developed to mimic *in vivo* natural extracellular microenvironments.[2] Recently, dynamic regulation of insoluble signaling ligands immobilized on extracellular matrices has attracted much attention because insoluble extracellular ligands such as integrin ligands in extracellular matrix molecules and notch ligands on the surface of neighbor cells are dynamically presented to cells in natural developmental and physiological processes.[3] Various stimuli-responsive strategies, such as pH, light, temperature, competition, and enzymes have been applied as triggers for presentation of bioactive ligands on the engineered materials.[4] Among all, light-stimuli received considerable attention because it can allow the noninvasively controlled presentation of bioactive ligands with relatively high spatial and temporal precision.[5] Compared with high UV/Vis light, near-infrared (NIR) light is expected to cause minimal normal tissue damage and has remarkably deep-tissue penetration.[6] NIR-absorbing nanoparticle is an appealing candidate for the application of NIR light to control presentation of bioactive ligands immobilized on the engineered materials because they can convert NIR light into heat by the photothermal effect. Several NIR-absorbing nanoparticles, such as gold nanorods (GNRs), gold nanoshells, gold nanocages, and graphene nanosheets, have been exploited for imaging, biosensing, photothermal therapy, and numerous other biomedical applications.[7] Among them, GNRs that have high electron density, excellent photothermal property,tunable localized surface plasmon resonance band from visible to NIR wavelength, and good biocompatibility have been extensively studied in both *in vitro* and *in vivo*.[8] In addition, engineered polypeptide biomaterials were widely reported to be utilized in biomedical applications.[9] The flexibility of recombinant DNA technology allows preparing of polypeptides with precise structures at the molecular level. Sequences of interest, such as binding domains, enzyme cleavage sites, and therapeutic peptides can be incorporated into engineered polypeptides. However, few approaches have been developed so far that incorporate an NIR-responsive GNRs with engineered polypeptides to reversible presentation of bioactive ligands on the engineered materials.

Herein, we developed a novel method for reversible presentation of the immobilized ligands to cell surface receptors by NIR light stimulus using polypeptide-engineered functionalized GNRs. In the molecular design illustrated in Scheme 1, bioactive ligands of interest are fused to one terminus of a leucine zipper A. GNRs are immobilized onto a mercaptosilane-modified glass substrate through a thiol-gold bond, followed by conjugation of polypeptide A fused with bioactive ligands to the GNRs. The immobilized ligand presents a cell-accessible state. The polypeptide A-functionalized GNRs allow coimmobilization of a B-PEG through a pair of complementary leucine zipper domains, which shields the bioactive ligands on the A and converts it to a cell-inaccessible state. An advantage of this design is that heterodimerization between A and B allows the bioactive ligands and PEG to be coimmobilized uniformly on the molecular level. To convert the ligand back to a cell-accessible state, coimmobilized B-PEG could be removed to release the shielded bioactive ligands through a photothermal mechanism of GNRs. Another advantage of this design is that the reversible regulation does not involve cleavage or immobilization of the ligand in the presence of cells, avoiding the potential detrimental effects of the non-immobilized ligand as a result of competitive binding for cell surface receptors. Thus, the design reported here may be used for tissue engineering and as tools for fundamental studies of cell behavior.

Britton Chance Center for Biomedical Photonics at Wuhan National Laboratory for Optoelectronics - Hubei Bioinformatics & Molecular Imaging Key Laboratory, Department of Biomedical Engineering, College of Life Science and Technology, Huazhong University of Science and Technology, Hubei, Wuhan 430074, P. R. China

E-mail: zydi@mail.hust.edu.cn (Y.-D. Zhao), lbyang@mail.hust.edu.cn (B. Liu); Fax: (+) 86 27-8779-2202

† Electronic Supplementary Information (ESI) available: Experimental details, amino sequences of polypeptides, SDS-PAGE, and photothermal effect of GNRs-ARGD-B-PEG. See DOI: 10.1039/c000000x/

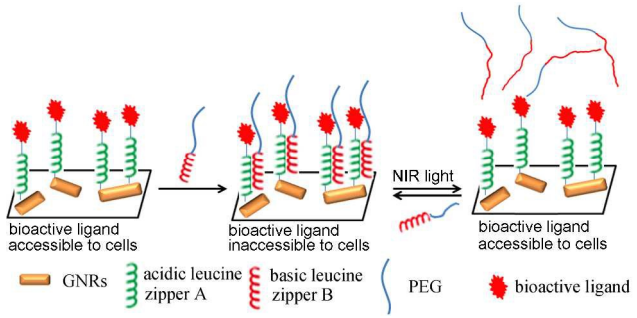

Scheme 1 Schematic illustration of reversible regulation of bioactive ligands presented on polypeptides-functionalized GNRs using NIR light.

The genetically engineered polypeptides used in this study were expressed in *E. coli* and purified as described previously (the sequences of cysA, cysARGD, and Bcys are shown in Supporting Information, Fig. S1).[10] The acidic leucine zipper domain A and the basic leucine zipper domain B can form a heterodimer with a high affinity (10^{-8}-10^{-10} M).[11] To shield the bioactive ligands on the A, B-PEG was prepared by modifying Bcys with excess PEG-dimaleimide or PEG-diacrylate. B-PEG was characterized using 12% SDS-polyacrylamide gel electrophoresis (Fig. S2). After conjugation with PEG, B-PEG retained its ability to form the heterodimer with the polypeptide A (Fig. 1a).

GNRs with dimensions of 44.7 ± 7.8 nm by 11.1 ± 0.9 nm (aspect ratio = 4) (Fig. 1b) and a longitudinal surface plasmon resonance (LSPR) at 800 nm (Fig. 1c) were prepared using the seed-mediated chemical synthesis method.[12] The ability of immobilization of polypeptide A onto the GNRs and the ability of polypeptides-functionalized GNRs to coimmobilize B-PEG through heterodimerization between A and B were examined. CysA or cysARGD was self-assembled on GNRs by means of gold-thiol bonds (Fig. 1c). The cell-adhesive RGD peptide ligand was chosen as a bioactive ligand and was fused on the polypeptide A. Characterization of the LSPR of the GNRs before and after polypeptides modification was performed by UV-vis spectroscopy. A large red-shift of approximately 80 nm for cysA and 110 nm for cysARGD was observed in maximal absorption peak, indicating that a dense polypeptide layer formed on the surface of GNRs. In addition, the LSPR was substantially broader, and the peak intensity decreased greatly after polypeptide functionalization. The loss of the longitudinal band in the NIR region is caused by aggregation when CTAB is replaced by the polypeptides.[13] The broadening of the longitudinal resonance wavelength may be due to electronic coupling between the GNRs-polypeptide at the longitudinal wavelength and/or to some aggregations of GNRs-polypeptide in solution.[14] Indeed, over time, obvious aggregations of the GNRs-polypeptide nanoparticles were observed. As expected, obvious blue-shift and narrowing of the LSPR were observed after binding with B-PEG, indicating that the B-PEG was successfully coimmobilized on the surface of GNRs through heterodimerization between A and B. Compared with GNRs, the LSPR of coimmobilized nanocomplexes (GNRs-ARGD-B-PEG) has a slight red-shift, which are probably related to the increased size of nanocomplexes. The stability of cysARGD-functionalized GNRs coimmobilization with B-PEG greatly improved than without because of hydrophilic PEG on the surface of GNRs.

To further confirm conjugation of the polypeptides on the surface of GNRs, the zeta potentials of GNRs and polypeptide-functionalized GNRs were measured (Fig. 1d). The first cysARGD or cysA conjugation step decreased the surface potential by 57.7 mV and 73.9 mV, respectively. The surface charges of polypeptides-functionalized GNRs changed from positive to negative because of glutamic acid and aspartic acid residues in the polypeptides, indicating that CTAB has been replaced by the polypeptides. The B-PEG coimmobilization step increased the zeta potential by 12.6 mV because the neutral PEG was coimmobilized on the surface of nanoparticles. The value of zeta potential of GNRs-ARGD-B-PEG decreased back after exposure to a continuous wave NIR laser (λ = 810 nm), suggesting that B-PEG was released from the GNRs-ARGD-B-PEG nanocomplexes due to denaturing of polypeptides. The GNRs-ARGD-B-PEG still presented high photothermal effect (Fig. S3). These results further demonstrate that GNRs-ARGD-B-PEG nanocomplexes were composed of a layer of thiolated ARGD and a layer of coimmobilized B-PEG, and B-PEG could be removed from the nanocomplexes through NIR light or heat.

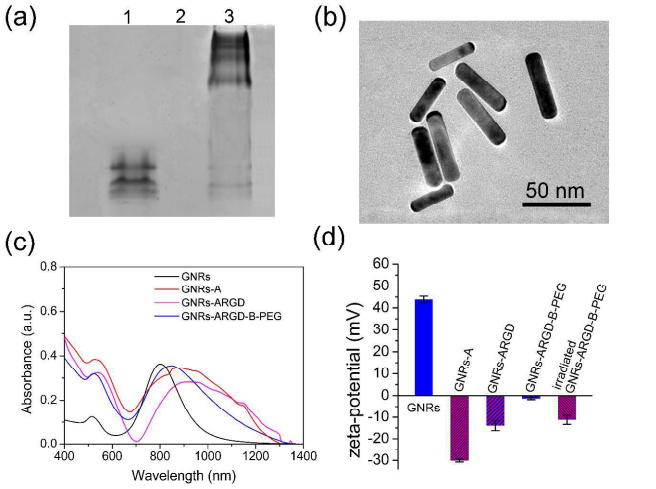

Fig. 1 (a) Native polyacrylamide gel electrophoresis of cysARGD (lane 1), B-PEG (PEG: 10 kDa) (lane 2), and their mixture (molar ratio of cysARGD:B-PEG 1:2) (lane 3). (b) TEM image of the GNRs. (c) The absorption spectra of GNRs, GNRs-A, GNRs-ARGD, and GNRs-ARGD-B-PEG. (d) Zeta-potential of GNRs and modified GNRs. Error bars present standard deviations of three experiments.

To test the ability of reversible regulation of bioactive ligands presented on immobilized GNRs in the presence of cells under physiological conditions, a two-dimensional system was designed (Scheme 1). First, GNRs were immobilized onto a mercaptosilanated glass substrate (Fig. 2a). The GNRs are randomly distributed on the substrate, and they appear to be parallel to the substrate. Although a large red-shift and broadening of the LSPR peak of immobilized GNRs compared to their spectrum in solution was observed (Fig. 2b), the absorbance at 810 nm was very strong. The red-shift is attributed to the greater refractive index of glass as compared to water and interparticle coupling.[15] CysARGD and cysA was each immobilized on the GNRs-modified glass substrate in the presence of 2 mM tris(2-carboxyethyl)phosphine hydrochloride (TCEP). Fibroblasts (NIH 3T3) were seeded on the substrate functionalized with GNRs and polypeptides and monitored with fluorescence microscopy. After 2 h, the cells efficiently attached and spread on the substrates modified with cysARGD (Fig. 3a), while few cells were observed on those functionalized with cysA (Fig. 3b). This result indicates that a single molecular layer of the polypeptides at the molecular level formed on the surface of GNRs. As expected, few cells were observed on the cysARGD-functionalized substrate after those incubated with B-PEG (MW of PEG: 10K) (Fig. 3c). The process from bioactive ligand accessible to cells to bioactive ligand inaccessible to cells indicates that the fused bioactive ligand on the

polypeptide A could be shielded by the PEG of coimmobilized B-PEG. Our previous studies have shown that shielding effect of B-PEG depended on the PEG size.[10] In order to shield different bioactive ligands fused on the polypeptide A, we only should choose different PEG sizes of B-PEG. Therefore, this system is universal because various bioactive ligands of interest can be incorporated into polypeptide A using the recombinant DNA technology.

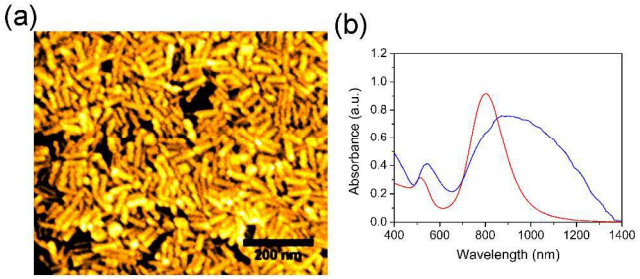

Fig. 2 (a) SEM of GNRs immobilized onto a glass substrate and (b) the absorption spectra of GNRs (red) and GNRs on glass substrate. Scale bar is 200 nm.

The switch that the cell-inaccessible RGD shielded by PEG could be converted back to the cell-accessible state by NIR light irradiation was further performed. After irradiation with 810 nm NIR laser at a power density of 3.0 W cm^{-2} for 4 min, the surface of substrate was converted from nonadhesive to cell-adhesive (Fig. 3d). It suggests that the coimmobilized B-PEG was removed by the phototermal effect of GNRs inducing denaturation of polypeptides. This result is in agreement with that obtained from zeta potentials. The melting temperature (Tm) of A domain is 40-55 ºC at different pH.[16] Previous studies have shown that few damage were obtained from cells treated with NIR light at low power density.[17] In addition, after irradiation with NIR light, the cell-accessible RGD could be reconverted to be cell-inaccessible by addition of B-PEG which is consistent with the result of our previous report.[10] These results indicate that the reversible switch of bioactive ligands fused on the polypeptide A on the surface of GNRs between cell-accessible and cell-inaccessible could be controlled by NIR light. Thus, this system can provide a noninvasive method for the reversible control cell adhesion using NIR light exposure under physiological conditions.

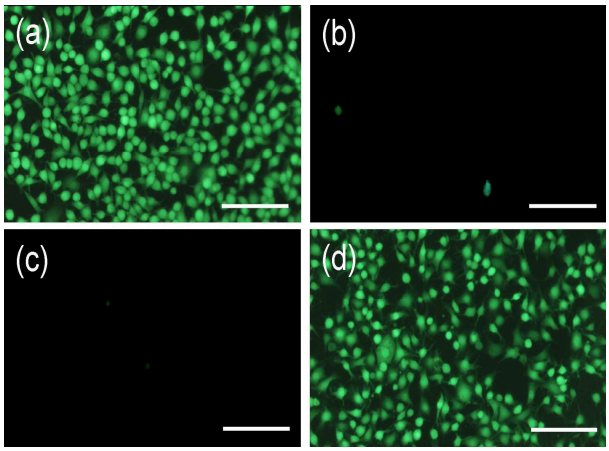

Fig. 3 Reversible presentation of immobilized RGD to cell surface receptors under physiological conditions. (a) The substrate modified with GNRs-ARGD. (b) The substrate modified with GNRs-A. (c) The substrate modified with GNRs-ARGD-B-PEG (PEG: 10 kDa). (d) The substrate modified with GNRs-ARGD-B-PEG (PEG: 10 kDa) after exposure to an 810 nm laser with a power density of 3.0 W cm^{-2} for 4 min. Scale bars are 200 μm.

The biocompatibility of polypeptides-functionalized GNRs nanoparticles was checked. Previous studies have shown that cetyltrimethylammonium bromide (CTAB) coated GNRs are toxic to many types of cells, which limits its applications in the fields of biomedicine.[18] The NIH 3T3 normal cells were grown in the presence of cysARGD, GNRs-ARGD, or GNRs-ARGD-B-PEG nanoparticles for 24 h, and the cell viabilities were assessed with MTT assay. As shown in Fig. 3, the viability of the HeLa cells decreased about 87% when they incubated with 40 μg/mL CTAB-GNRs, which is consistent with the previously reported results.16 Compared to CTAB-GNRs, cysARGD-functionalized GNRs showed improved biocompatibility toward cells. This may be attributed to toxic CTAB replaced by the nontoxic polypeptide. The cell viabilities of GNRs-ARGD-B-PEG were not significantly different from control cells. The excellent biocompatibility of GNRs-ARGD-B-PEG is most likely due to the stability and surface charge of particles offered by the PEG.[19]

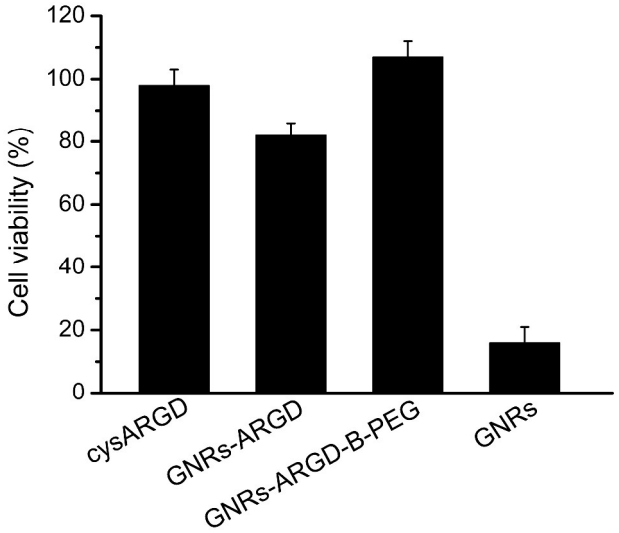

Fig. 4 *In vitro* viability of NIH 3T3 cells treated with free cysARGD polypeptide, CTAB-GNRs, GNRs-ARGD, and GNRs-ARGD-B-PEG (PEG: 10 kDa). The concentration of the free cysARGD polypeptide is 20 μM, and the concentration of CTAB-GNRs, GNRs-ARGD, and GNRs-ARGD-B-PEG are 40 μg mL^{-1}.

In summary, a new system of dynamic presentation of immobilized ligands was fabricated by the NIR light control using GNRs functionalized with engineered polypeptides. A polypeptide fusion of bioactive ligands of interest and a leucine zipper domain A and a conjugation of PEG and another leucine zipper domain B (B-PEG) were subsequently modified on the GNRs. Heterodimerization between A and B allows coimmobilization of PEG, which shields bioactive ligands on the A. When the functionalized GNRs were irradiated by 810 nm NIR light, the coimmobilized B-PEG was removed, and the bioactive ligands were presented again to the receptor of cells. Precise regulation is assured by the molecular-level uniformity of coimmobilization conferred by the molecular recognition between A and B. Therefore, the method reported here for the presentation of the bioactive ligands to the cell surface receptors is reversible. This GNRs-based photoswitchable system may find applications in different areas of cell biology and biomedicine, such as cell adhesion/detachment, cell migration, stem cell differentiation, cell-based drug screening and drug delivery.

This work was supported by the National Key Technology R&D Program of China (2012BAI23B02), the National Natural Science Foundation of China (Grant No. 81471697, 31100704, 81271616), the Foundation for Innovative Research Groups of the NNSFC (Grant No. 61121004), and the Open Research Fund of Collaborative innovation center of modern bio-manufacture, Anhui University. The authors thank Prof. David Tirrell generously providing PQE9PC$_{10}$A plasmid. We also thank the facility support of the Center for Nanoscale Characterization and Devices, Wuhan National Laboratory for Optoelectronics (WNLO) and Analytical and Testing Center (HUST).

Notes and references

1 P. M. Kharkar, K. L. Kiick and A. M. Kloxin, *Chem. Soc. Rev.* 2013, **42**, 7335-7372.

2 a) J. J. Rice, M. M. Martino, L. D. Laporte, F. Tortelli, P. S. Briquez and J. A. Hubbell, *Adv. Healthec. Mater.* 2013, **2**, 57-71; b) J. Kopecek and J. Yang, *Angew. Chem. Int. Ed.* 2012, 51, 7396-7417.

3 a) M. P. Lutolf and J. A. Hubbell, *Nat. Biotechnol*. 2005, **23**, 47-55; b) S. Artavanis-Tsakonas, M. D. Rand and R. J. Lake, *Science* 1999, **284**, 770-776.

4 a) W. Zheng, W. Zhang and X. Jiang, *Adv. Healthec. Mater.* 2013, **2**, 95-108; b) S. R. Meyers and M. W. Grinstaff, *Chem. Rev.* 2012, **112**, 1615-1632; c) D. Shin, J. H. Seo, J. L. Sutcliffe and A. Revzin, *Chem. Commun* 2011, **47**, 11942-11944; d) P. M. Mendes, *Chem. Soc. Rev.* 2008, **37**, 2512-2529.

5 T. Kuo, V. A. Hovhannisyan, Y. Chao, S. Chao, S. Chiang, S. Lin, C. Dong and C. Chen, *J. Am. Chem. Soc.* 2010, **132**, 14163-14171.

6 a) W. Li, J. Wang, J. Ren and X. Qu, *Angew. Chem. Int. Ed.* 2013, 52, 6726-6730; b) J. You, J. S. Heo, J. Kim, T. Park, B. Kim, H. Kim, Y. Choi, H. O. Kim and E. Kim, *ACS Nano* 2013, **7**, 4119-4128.

7 V. Biju, *Chem. Soc. Rev*. 2014, **43**, 744-764.

8 a) X. Huang, H. El-Sayed, W. Qian and M. A. El-Sayed, *J. Am. Chem. Soc.* 2006, **128**, 2115-2120; b) B. Wang, J. Wang, Q. Liu, H. Huang, M. Chen, K. Li, C. Li, X. Yu and P. K. Chu, *Biomaterials* 2014, **35**, 1954-1966. c) C. Yu, Z. Zhu, Q. Wang, W. Gu, N. Bao and H. Gu, *Chem. Commun* 2014, **50**, 7329-7331.

9 a) Y. Tian, H. Wang, Y. Liu, L. Mao, W. Chen, Z. Zhu, W. Liu, W. Zheng, Y. Zhao, D. Kong, Z. Yang, W. Zhang, Y. Shao and X. Jiang, *Nano Lett.* 2014, **14**, 1439-1445; b) C. C. Huang, S. Ravindran, Z. Yin and A. George, *Biomaterials*, 2014, **35**, 5316-5326; c) H. Wang, Y. Shi, L. Wang and Z. Yang, *Chem. Soc. Rev*. 2013, **42**, 891-901.

10 B. Liu, Y. Liu, J. J. Riesberg and W. Shen, *J. Am. Chem. Soc.* 2010, **132**, 13630-13632.

11 a) W. Shen, K. C. Zhang, J. A. Kornfield and D. A. Tirrell, *Nat. Mater.* 2006, **5**, 153-158; b) B. Liu, Y. Liu, A. K. Lewis and W. Shen, *Biomaterials* 2010, **31**, 4918-4925.

12 B. Nikoobakht and M. A. El-Sayed, *Chem. Mater*. 2003, **15**, 1957-1962.

13 a) M. Sethi, G. Joung and M. R. Knecht, *Langmuir* 2009, **25**, 1572-1581; b) H. Huang, S. Barua, D. B. Kay and K. Rege, *ACS Nano* 2009, **3**, 2941-2952; c) H. Huang, A. Nanda and K. Rege, *Langmuir* 2012, **28**, 6645-6655.

14 M. D. Bkankschien, L. A. Pretzer, R. Huschka, N. J. Halas, R. Gonzalez and M. S. Wong, *ACS Nano* 2013, **7**, 654-663.

15 S. M. Marinakos, S. Chen and A. Chilkoti, *Anal. Chem.* 2007, **79**, 5278-5283.

16 W. A. Petka, J. L. Harden, K. P. McGrath, D. Wirtz and D. A. Tirrell, *Science* 1998, **281**, 389-392.

17 a) Z. Li, P. Huang, X. Zhang, J. Lin, S. Yang, B. Liu, F. Cao, P. Xi, Q. Ren and D. Cui, *Mol. Pharm.* 2009, **7**, 94-104; b) S. Shen, H. Tang, X. Zhang, J. Ren, Z. Pang, D. Wang, H. Gao, Y. Qian, X. Jiang and W. Yang, *Biomaterials*, 2013, **34**, 3150-3158.

18 a) A. P. Leonov, J. Zheng, J. D. Clogston, S. T. Stern, A. K. Patri and A. Wei, *ACS Nano* 2008, **2**, 2481-2488; b) A. M. Alkilany, P. K. Nagaria, C. R. Hexel, T. J. Shaw, C. J. Murphy and M. D. Wyatt, *Small* 2009, **5**, 701-708; c) X. Huang, S. Neretina and M. A. El-Sayed, *Adv. Mater.* 2009, **21**, 4880-4910.

19 L. Wang, X. Jiang, Y. Ji, R. Bai, Y. Zhao, X. Wu and C. Chen, *Nanoscale* 2013, **5**, 8384-8391.

